CUMULATIVE DAMAGE OF WELDED BEAM-TO-COLUMN CONNECTIONS IN STEEL STRUCTURES SUBJECTED TO DESTRUCTIVE EARTHQUAKES

Kiyoshi KANETA (I)
Isao KOHZU (II)
Hidekazu NISHIZAWA (II)
Presenting Author: Isao KOHZU

SUMMARY

In order to assess aseismic safety of welded structures subjected to destructive earthquakes, based upon the concept of low cycle fatigue failure, this paper deals with the characteristics of low cycle fatigue of welded beam-to-column connections which were tested statically and dynamically under repeated loading conditions. From these experimental results, it has been recognized that low cycle fatigue damage of welded steel structures against destructive earthquakes can be well predicted by employing the proposed method derived from the statically loading test results.

INTRODUCTION

Moment registing steel structures are well recognized as one of the most aseismic structures, because of good deformability beyond the elastic range and large amount of the energy absorbing capacity that the materials can possess. However, a large number of cyclic deformations in the inelastic range which the structures would suffer in the event of destructive earthquakes, may considerably result in a failure so-called the low cycle fatigue phenomenon at the critical sections in the structures.

From this point of view, it is necessary to make clear low cycle fatigue property of the materials, the subassemblages bolted or welded, and the whole structures, when the structures are subjected to such major earthquakes. Since the welded structures are commonly used in the current design practice, the inelastic behavior of the welded connections like as the beam-to-column connections, becomes the most important factor to assess aseismic safety of the structures. For this reason, this paper is focussed to the clarity of low cycle fatigue property and fatigue damage estimation of the welded beam-to-column connections due to earthquakes, based on the statical as well as the dynamical experiments.

STATIC LOADING TESTS

Specimens

Hot rolled sections H-200x100x5.5x8 and H-200x200x8x12 (unit; millimeter) made of the JIS SS41 grade steel were used for the beam and the column members, respectively. The coupon test results of the material used for the beam flange are shown in Table 1.

(I) Professor of Structural Engineering, Kyoto University, Kyoto, Japan

(II) Research Assistant, ditto

The welding of the beam-to-column connection was performed by means of the manual arc welding in the manner of which the web of the beam was fillet welded to the column flange and thereafter, each flange of the beam was butt welded to the column flange.

The specimens were classified into the following two series.

a) Series A

The specimens belonging to Series A were the cantilever type specimens of the same shape like those which had been tested by Popov et al.(Ref. 1), as shown in Fig.1. These specimens were further classified into three types, A1 to A3 types, according to the combinations of the programmed tip deflections and the welding procedures at the beam ends. For A1 and A2 type specimens, the beam flanges were single bevel butt welded with backing strips to the column flanges. For A3 type specimens, the beam flanges were butt welded with back run.

b) Series B

The specimens of Series B were fabricated as shown in Fig.2. The members of each specimen consisted of the two beams and the stub column connected to the beams at the center of the specimen. The panel of the column was stiffened by the doubler plates so as to prevent the shear deformations of the panel zone.

These details of the groove shapes are illustrated in Fig.3.

Procedures of the Experiments

The column of the cantilever type specimen was connected rigidly with high strength bolts to a reaction frame and the beam was loaded cyclically at the tip so as to generate the large bending moment at the beam end. The tip deflection of the beam was measured by an extensometer and the cyclic test was carried out in the manner to control the magnitude of the deflection as described later. The general view of the test set-up is illustrated in Fig.4. For the specimen of Series B, an universal loading machine was applied to load cyclically at the center of the specimen, by controlling the deflection at the center detected by an extensometer. The general view of the test set-up is shown in Fig.5. In addition, several wire strain gauges were pasted to the flange of the beam at or near the beam end, and they were continuously recorded on a digital strainmeter during the experiment.

Programmed deflection patterns consisted of two types, which were perfectly reversed types with and without mean deflections, and the combinations of the deflection patterns and the specimens were tabulated in Table 2 with the number of loading cycles repeated at the programmed deflection amplitudes or those to failure.

Test Results

The results of cyclic loading tests for the specimens indicated that the load-deflection curves and the local strain outputs stabilized at about 2 or 3 initial cycles and after many cyclic loadings the cracks initiated at the intersections of the beam flanges and the scallops, or at the welded connections of the beam flanges, and propagated along the directions of the flange

widths, as illustrated in Fig.6. It could be observed from the test results that the cyclic tests controlled by the deflection amplitudes at the tips or the centers of the specimens become equivalent to the strain controlled tests of the flanges at or near the beam ends and fracture patterns of every specimens do not depend upon the details of the connections and the magnitudes of the deflection amplitudes.

Predictions of the Fatigue Lives

a) Experimental Formula for Perfectly Reversed Loading Test Results without Mean Deflections

Since the mechanical properties of the materials are different from each other, their influence upon the fatigue life must be taken into consideration. For this reason, a method has been proposed to use the normalized plastic strain range instead of the directly measured plastic strain range, $\Delta\varepsilon_p$, in the following way: Assume that the initial stiffeness remains unchanged until the point at which the beam end arrives at the fully plastic moment, M_p, then the corresponding plastic strain, ε_p, can be computed using the relation, $M_p/M_y = \varepsilon_p/\varepsilon_y$, in which M_y is the bending moment of the beam when the fibers of the flanges arrive at the yield strain, ε_y. Therefore, the non-dimensional plastic strain range, $\Delta\varepsilon_p/\varepsilon_p$, can be evaluated.

For the test results under the fully reversed constant deflection amplitudes without mean deflections, the relation between the non-dimensional plastic strain ranges and the corresponding fatigue lives can be formulated as follows by employing the least squares method.

$$\frac{\Delta\varepsilon_p}{\varepsilon_p} = 71 \cdot (N_f)^{-0.57} \qquad (1)$$

In this equation, the plastic strain range, $\Delta\varepsilon_p$, was measured from the bending moment-averaged strain curve at the point of the beam from which the web was scalloped.

b) Fatigue Life Predictions for the Test Results under the Multi Step Deflection Amplitudes and the Amplitudes with Mean Deflections

A simplified prediction method refered to the hypotheses proposed by Miner, Weiss and other authors, was adopted to count the low cycle fatigue damage under varying strain amplitudes. Initially, it is assumed that cumulative damage can be estimated by linear summation of individual damage under constant strain amplitudes which can be defined as n_i/N_{fi}, in which n_i is an actual number of cycles under a constant strain amplitude, and N_{fi} is the number of cycles to failure under the corresponding constant strain amplitude. Since N_{fi} is calculated from Eq.(1), cumulative damage, DF, can be formulated as follows:

$$DF = \sum_i \frac{n_i}{N_{fi}} = \sum_i \frac{n_i}{\left(\frac{1}{K} \cdot \frac{\Delta\varepsilon_p}{\varepsilon_p}\right)^{\frac{1}{0.57}}}, \text{ in which } K = 71 \qquad (2)$$

When the mean strain has to be taken into consideration, K value of Eq.(2) is substituted by K' as follows.

$$K' = K \cdot \left(1 - \frac{\varepsilon_m}{\bar{\varepsilon}} \right) \tag{3}$$

in which ε_m is the mean strain and $\bar{\varepsilon}$ represents the value of $\Delta\varepsilon_p$ which can be obtained by substituting N_f in Eq.(1) for $1/2$.

The computed results of the damage factors to failure for an individual specimen can be obtained as summarized in Table 3. From this table, it can be recognized that the estimate of fatigue lives under varying strain amplitudes can be assessed within the safety region by assuming that fatigue failure happens when the value of damage factor arrives at 0.5.

DYNAMIC LOADING TESTS

Specimens and Test Structures

In order to simulate the dynamic behavior in an actual weak beam-strong column type steel structure and the low cycle fatigue failure at the beam-to-column connection in the event of destructive earthquakes, a simple structure model was fabricated and tested on a shaking table by applying two types of excitations to the structure-shaking table system.

Geometry of the specimen used for this experiment is shown in Fig.7. The material was made of JIS SS41 grade steel. The mechanical properties of the plates used for the beam were obtained from the coupon test and the results are summarized in Table 4. The beam flange was single bevel butt welded with backing strip and the web was fillet welded to the column flange. The panel zone of the beam-to-column connection was stiffened by the doubler plates to prevent the shear deformation, and their detail is also shown in Fig.7.

A same column member as that of the specimen was used to form a complete frame structure together with the specimen and was pin-jointed to the free end of the beam. Two identical plane frames were spaced about 1.5 m apart and were erected so as to form a three dimensional one bay-one story steel structure on the shaking table. The column bases of the structure were pin-jointed to the steel footings fastened to the shaking table. The structure was reinforced at the both side elevations by angle bracings, and concrete blocks weighing about 1.35 tons connected rigidly to the roof beams were supported by the removable transverse beams so that the beams of the specimens could not be subjected to the vertical loads carried from the concrete blocks.

The beam of the specimen was supported by the cross beams at the third points to prevent lateral buckling. In addition, the roof was stiffened by diagonal braces of the tension rods in order to prevent torsional oscillations of the structure.

Procedures of the Experiments

The shaking table driven by an electro-magnetic type shaker, which was of capacity as listed in Table 5, was used to generate the horizontal excitations

in only one direction.

Accelerometers were mounted on the tops of the columns of the specimens and the shaking table to measure the absolute accelerations. In addition, the absolute displacements of the structure and the shaking table were measured by displacement transducers connected to rigid steel frames which were erected on the concrete basement. The set-up of the test structure and the measuring instruments is illustrated in Fig.8. Local strains at or near the beam-to-column connection were detected by post yield type strain gauges cemented to the beam flanges. All data obtained from these measuring instruments were recorded to the magnetic tapes set up in analog data recorders during the experiment and at the same time, the outputs of such data were monitored on a pen oscillograph.

At first, the structures were subjected to sinusoidal excitations with the very small magnitudes, in order to measure the elastic dynamic properties of the structures such as the natural frequencies of vibrations and the damping factors. Table 6 shows the results of these dynamic properties of the test structures.

Two types of the shaking table motions were used to cause low cycle fatigue failure to the structures. One of the input motions was steady sinusoidal motions with the frequencies close to the fundamental natural frequencies of the structures of Series C. The input motions whose intensities were kept constant at about $0.5g$, were applied repeatedly to the system until the critical sections of the specimens fractured. As another type of input motions, the earthquake motion derived from the NS component of the 1952 Taft earthquake record, was modified regarding the time intervals and the intensities, and was applied to the system. The structure used for this experiment was named as Series D. The procedure of this experiment was intended so that the system would suffer the modified earthquake excitations step by step with gradual increase of the intensity up to about $1.0g$, and in subsequent tests, the input motions with the constant intensity of about $1.0g$ would be applied over and over again until the specimens would have fractured.

Test Results

The results of the sinusoidal vibration test and the earthquake motion test were summarized in Tables 7 and 8, respectively. The fractures of every specimens occurred at the flanges of the beam ends located at the points from which the webs were scalloped. Such phenomenon was the same as that observed from the results of the statically loading test.

Typical groval and local normalized responses of the structure subjected to the modified earthquake motions are shown in Fig.9. The strain responses, as shown in the lower three figures of Fig.9, demonstrate the yielding and the subsequent strain drifts significantly at the 8th step of the test. From the bending moment-local strain diagram at the critical section of the beam at the 19th step of the test, as shown in Fig.10, it can be observed that the nonlinear responses are evidently developed as the test becomes close to the final step.

Evaluation of Low Cycle Fatigue Damage

To inspect the validity of the formerly described method to estimate the low cycle fatigue damage under varying strain histories, the strain responses at the beam ends measured during the dynamic tests were used to account the low cycle fatigue damage of the structures.

For the sinusoidal excitation tests, Eqs.(2) and (3) were employed to compare the expected damages with the test results. For the earthquake motion test, Eqs.(2) and (3) as well as a counting method so-called as the Rain Flow Counting Method, which were proposed by Suidan et al.(Ref. 2), were applied to estimate random low cycle fatigue damage by substituting the varying strain histories to the group of the equivalent steady strain responses with mean strains.

These computed results are shown in Table 9. Since the computed values in Table 9 does not indicate the significant difference in comparison with the values in Table 3, it can be seen that the proposed method to predict low cycle fatigue damage under statically varying strain histories is available for the damage estimation under dynamic strain histories like as actual earthquakes.

CONCLUSIONS

Low cycle fatigue properties under constant and varying strain histories were investigated using the steel beam and column subassemblages, statically as well as dynamically. From the test results, the following conclusions have been drawn:

1. At the beam-to-column welded connection in the weak beam-strong column type steel structure, the beam flange from which the web is scalloped may become the most critical point to cause low cycle fatigue failure due to cyclic loadings.

2. Low cycle fatigue failure of the beam-to-column connection under constant strain amplitudes can be formulated using the non-dimensional plastic strain ranges at the critical point and the cycles to failure. Cumulative fatigue damage under varying strain histories can be estimated, employing this experimental formula and the linear damage law, and the safety of the connection can be assessed by assuming that the fracture occurs when the computed cumulative damage factor arrives at the value, 0.5.

3. The proposed method is also available for damage estimation in the steel structure due to destructive earthquakes, by further employing the Rain Flow Counting Method.

REFERENCES

(1) Popov, E. P., and Bertero, V. V., "Cyclic Loading of Steel Beams and Connections," J. of the Structural Division, ASCE, Vol.99, No.ST6, June, 1973, pp.1189-1204.
(2) Suidan, M. T., and Eubanks, R. A., "Cumulative Fatigue Damage in Seismic Structures," J. of the Structural Division, ASCE, Vol.99, No.ST5, May, 1973, pp.923-943.

Table 1 COUPON TEST RESULTS OF SERIES A AND B

	SPECIMEN TYPE		
	A_1	A_2, B	A_3
YIELD STRESS σ_y (t/cm^2)	2.78	2.88	3.33
TENSILE STRENGTH σ_u (t/cm^2)	4.10	4.63	4.65
YIELD STRAIN ε_y (%)	0.130	0.135	0.162
ELONGATION ε_u (%)	27.8	30.4	29.8
YOUNG'S MODULUS E (t/cm^2)	2138	2133	2056

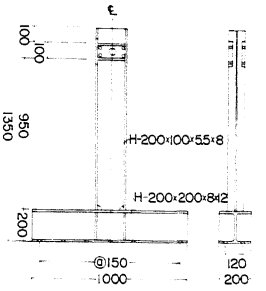

(Unit: mm)

Fig.1 SPECIMEN (SERIES A)

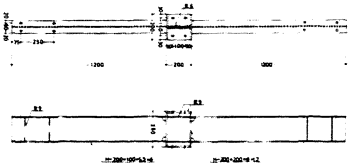

(Unit: mm)

Fig.2 SPECIMEN(SERIES B)

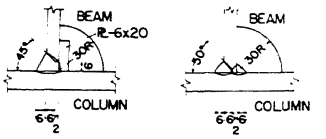

TYPE A_1, A_2 AND B TYPE A_3

Fig.3 DETAILS OF GROOVE SHAPES

Table 2 PROGRAMMED DEFLECTIONS AND NUMBER OF CYCLES

SPECIMEN	PROGRAMMED DEFLECTION AMPLITUDE (cm)
A_1 - 1	±1.26(53) [0.0]
A_1 - 2	±1.00(189) [0.0]
A_1 - 3	±0.74(605) [0.0]
A_2 - 1	±0.74(20) → ±1.00(10) → ±1.26(10) ±1.52(10) → ±1.78(6) [0.0]
A_2 - 2	±0.74(20) [0.37] → ±1.00(10) [0.5] ±1.26(10) [0.63] → ±1.52(10) [0.76] ±1.76(5) [0.89]
A_2 - 3	±1.78(10) → ±1.52(10) → ±1.26(10) ±1.00(7) [0.0]
A_2 - 4	±0.74(3) → ±1.00(3) → ±1.26(3) → ±1.52(3) ±1.78(3) → ±1.52(3) → ±1.26(3) → ±1.00(3) ±0.74(3) → ±1.00(3) → ±1.26(3) → ±1.52(3) ±1.78(3) → ±1.52(3) → ±1.26(3) → ±1.00(3) ±0.74(3) → ±1.00(3) → ±1.26(3) → ±1.52(3) ±1.78(3)
A_2 - 5	±1.00(10)[0.0] → ±1.00(10)[0.5] ±1.00(10)[1.0] → ±1.00(10)[0.5] ±1.00(10)[0.0] → ±1.00(10)[-0.5] ±1.00(10)[-1.0] → ±1.00(10)[-0.5] ±1.00(10)[0.0] → ±1.00(10)[0.5] ±1.00(10)[1.0] → ±1.00(10)[0.5] ±1.00(10)[0.0] → ±1.00(10)[-0.5] ±1.00(10)[-1.0]
A_3 - 1	±1.26(127) [0.0]
A_3 - 2	±1.52(51) [0.0]
A_3 - 3	±1.00(211) [0.0]
A_3 - 4	±1.26(94) [0.0]
A_3 - 5	±1.78(39) [0.0]
B - 1	±1.68(32) [0.0]
B - 2	±1.00(135) [0.0]
B - 3	±0.60(20) → ±1.00(10) → ±1.68(10) ±0.60(20) → ±1.00(10) → ±1.68(10) [0.0]
B - 4	±1.68(10) → ±1.00(10) → ±0.60(20) ±1.68(7) [0.0]
B - 5	±2.30(4) → ±1.68(8) → ±2.30(4) [0.0]

( ): NUMBER OF CYCLES, [ ]: MEAN DEFLECTION

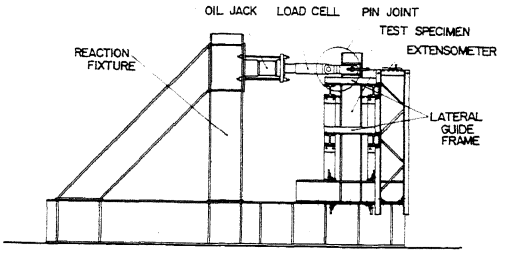

Fig.4 SET-UP OF LOADING APPARATUS FOR SERIES A

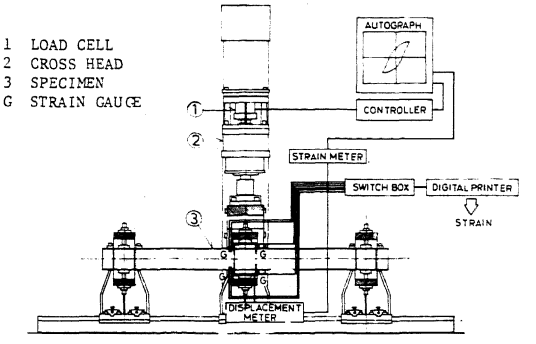

Fig.5 SET-UP OF LOADING APPARATUS FOR SERIES B

Table 3 COMPUTED DFS OF SERIES A AND B

SPECIMEN	DF
A -1	0.82
A -2	0.67
A -3	0.84
A -4	0.85
A -5	0.67
B -3	0.86
B -4	0.59
B -5	0.72

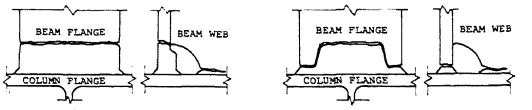

TYPE A_1, A_2 AND B TYPE A_3

Fig.6 FRACTURE PATTERNS

Table 4 COUPON TEST RESULTS OF BEAM FLANGES (SERIES C AND D)

	SERIES	
	C	D
YIELD STRESS σ_y (t/cm²)	3.53	3.95
TENSILE STRENGTH σ_u (t/cm²)	5.17	5.10
YIELD STRAIN ε_y (%)	0.168	0.191
YOUNG'S MODULUS E (t/cm²)	2101	2113

Table 5 SPECIFICATIONS OF SHAKING TABLE

EXCITING FORCE (t)	4.0
FREQUENCY RANGE (Hz)	0.2~200
MAXIMUM STROKE(mm)	±50
ALLOWABLE LOAD (t)	5.0
TABLE SIZE (m)	2.5x2.5
TABLE WEIGHT (t)	3.0

Table 6 ELASTIC DYNAMIC PROPERTIES

	NATURAL FREQUENCY (Hz)	DAMPING FACTOR (%)
SERIES C	4.0	1.8
SERIES D	3.7	1.5

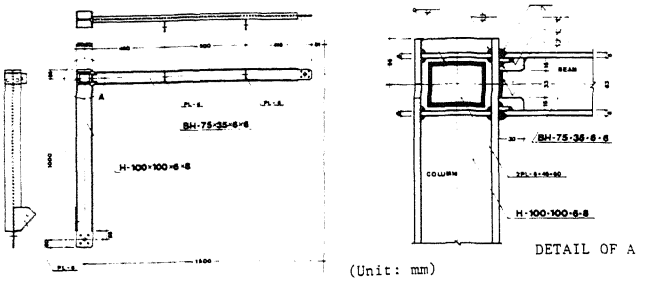

(Unit: mm)

Fig.7 SPECIMEN (SERIES C AND D)

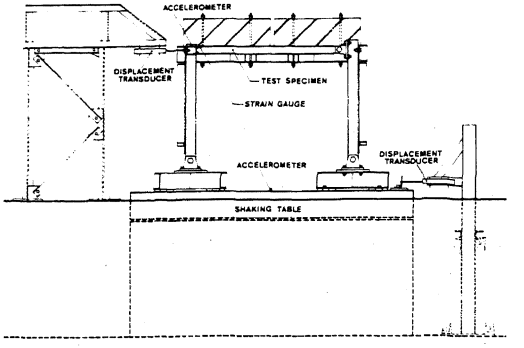

Fig.8 TEST SET-UP OF DYNAMIC LOADING TEST

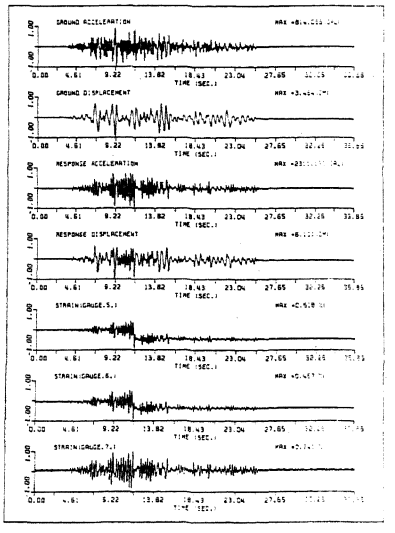

Fig.9 TIME HISTORIES (SERIES D, THE 8TH STEP)

Table 7 TEST RESULTS OF SERIES C

TYPE	INPUT MOTION		RESPONSES		
	FREQUENCY (Hz)	INTENSITY (gal)	INTENSITY (gal)	$\Delta\varepsilon_0$ (%)	N_f (cycles)
C_1	3.3	500	1928	0.77	115
C_2	3.0	400	1239	0.133	160
	3.0	500	1428	0.413	172
	3.0	500	1445	0.71	71

Table 8 TEST RESULTS OF SERIES D

STEP	1 ~ 5th	6 ~ 8th	9 ~ 20th
INTENSITY OF INPUT M. (gal)	104 ~ 478	675 ~ 830	986
INTENSITY OF ROOF M. (gal)	264 ~ 1322	1453 ~ 2220	2643
MAXIMUM STRAIN* (%)	0.033 ~ 0.200	0.317 ~ 0.965	1.663 ~ 1.720

* measured from the first step

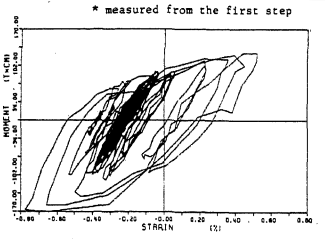

Fig.10 MOMENT-STRAIN DIAGRAM AT THE BEAM END (SERIES D, THE 19TH STEP)

Table 9 COMPUTED DFS OF SERIES C AND D

TYPE	DF
C_1	0.87
C_2	0.82
D	0.58